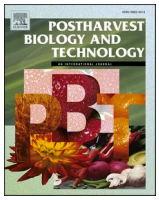
Postharvest Biology and Technology 212 (2024) 112878



Contents lists available at ScienceDirect

Postharvest Biology and Technology

journal homepage: www.elsevier.com/locate/postharvbio





Non-destructive methods for mango ripening prediction: Visible and near-infrared spectroscopy (visNIRS) and laser Doppler vibrometry (LDV)

C. O'Brien, N. Falagán, S. Kourmpetli, S. Landahl, L.A. Terry, M.C. Alamar *

Plant Science Laboratory, Cranfield University, Cranfield MK43 0AL, UK

ARTICLE INFO

Keywords:
Mangifera indica
Firmness
Food loss
Chemometrics
Resonant frequency
Postharvest

ABSTRACT

With up to 19% of mango fruit being lost during ripening, the need for non-destructive technologies to predict internal physiochemical traits is paramount. This study compared two non-destructive technologies, visible and near-infrared spectroscopy (visNIRS) and laser Doppler vibrometry (LDV), for predicting the ripeness of mango fruit in two cultivars, 'Kent' and 'Keitt'. An internal quality index (IQI) in 'Kent' was predicted using visNIRS (R^2_P = 0.729, RMSEP = 0.532) using partial least squares regression, which gave a single measure for ripeness incorporating firmness, sweetness, and pulp colour. This model was improved by using the sum of the individual sugar contents (glucose, sucrose, and fructose) over the conventional total soluble solids (TSS) measure. LDV provided poor predictions of firmness ($R^2 < 0.5$) in both 'Kent' and 'Keitt' using least squares regression line. The resonant frequency, as measured by LDV, decreased linearly with time, while firmness quantified destructively (quasi-static) showed an exponential decrease, suggesting the vibrational and destructive firmness measure distinct characteristics, which would contribute to poor model performance. These results showed that LDV is not suitable for assessing mango ripening. While visNIRS models have been successful at predicting quality traits, our results suggested that using individual sugar content in place of TSS can improve the prediction of ripening. This understanding of the strengths and limitations of both visNIRS and LDV, and how they relate to destructive quality measurements, can be used to improve postharvest management practices whilst reducing commercial losses in the mango industry.

1. Introduction

During the postharvest ripening process in mango, losses can reach up to 19% (FAO, 2018). Physical losses can occur due to over-ripening (past consumer acceptability), while processing too early (e.g. peeling and cutting for the fresh-cut market) causes quality and nutritional losses (FAO, 2018; Liu et al., 2020; Silué et al., 2022). Reducing these losses is paramount for sustainable food systems. Ripening is a complex trait that involves many physicochemical changes including colour, firmness, sugars, and volatiles (Silva et al., 2008; Zaharah et al., 2012; Lebrun et al., 2008). Preharvest factors (including differences in flowering time, canopy position, and irrigation) can lead to high heterogeneity in mango fruit development and postharvest behaviour. This inherent heterogeneity within batches means that a large number of fruit needs to be assessed to obtain representative data. Knowing the ripening stage of a batch allows for better postharvest management practices, including optimising the storage duration and conditions.

Across the industry, destructive methods are used to estimate mango ripeness. For example, penetrometers, can measure mango firmness (Hernández Gómez et al., 2005; Padda et al., 2011), but each fruit measured is then not marketable due to the puncture. Another destructive measurement is TSS, frequently used to estimate soluble sugar content in fresh produce (Munawar et al., 2013), and has been shown to correlate well with sweetness in 'Keitt' mangoes (Silva et al., 2008). However, TSS is an optical density measurement that does not always correlate well with sugar content (Harker et al., 2002; Hale et al., 2005; Beckles, 2012) as it also includes soluble proteins and organic acids (Kusumiyati et al., 2020). However, it is generally accepted that a dominant factor in sweetness is the concentration of sugars (Moskowitz, 1970; Helstad, 2019; Mouillot et al., 2019), which in mango are sucrose, fructose, and glucose (Silva et al., 2008).

Replacing destructive measurements commonly used in industry to assess internal quality with non-destructive methods is necessary for reducing commercial losses. Non-destructive assessments are also needed to allow the analysis of increased numbers of fruit per batch to better account for heterogeneity, and thus improve quality

* Corresponding author.
E-mail address: m.d.alamargavidia@cranfield.ac.uk (M.C. Alamar).

https://doi.org/10.1016/j.postharvbio.2024.112878
Received 14 September 2023; Received in revised form 12 January 2024; Accepted 5 March 2024
Available online 16 March 2024
0925-5214/© 2024 The Authors. Published by Elsevier B.V. This is an open access article under the CC BY license (http://creativecommons.org/licenses/by/4.0/).

management. This alternative will also decrease the nutritional and quality losses associated with processing or eating the fruit at non-optimal ripening stages.

Visible and near-infrared spectroscopy (visNIRS) has been widely used to predict physico-chemical properties of fresh produce (e.g. TSS, dry matter content, acidity; Supplementary Table 1), and has been shown to be effective in a wide range of fruit species, including mango. VisNIRS has also allowed for the prediction of quality indices such as maturity index, ripening index, and internal quality index (IQI; **Equation 1**). These indices incorporate several traits, such as firmness, shape, dry matter content, TSS, acidity, and colour, into a single measure (Cortés et al., 2016; Cortés, et al., 2017; Munera et al., 2017, 2019; Gupta et al., 2021). Using a single, comprehensive measure, such as IQI, simplifies the ripeness assessment.

There are, however, several drawbacks to visNIRS for the prediction of quality attributes. VisNIRS models generally do not perform well on fruit from different origins and seasons, when only trained on a single harvest, due to high biological variability (Bobelyn et al., 2010; Rungpichayapichet et al., 2016). VisNIRS is also sensitive to changes in temperature, predominantly due to the changes in OH and CH bonds in biological materials (Golic et al., 2003).

Additionally, visNIRS gives information related to only a single 'point' on the fruit (ranging *ca.* 2–20 mm diameter), as opposed to hyperspectral imaging, which can give distinct measurements for each pixel of the 2D image, typically covering most of the surface area of the fruit (Walsh et al., 2020). This means that the physical and chemical gradients that exist within the product are not well represented, or require additional time and resources for repeated measures in each fruit to be acquired in order to be more representative. Ripening in mango is known to lead to heterogeneity within the pulp in attributes including colour and biochemical composition (Thanaraj et al., 2009, Nordey et al., 2014).

Laser Doppler vibrometry (LDV) measures the vibrations of an object and can relate the resonant frequency (*f*) with the fruit texture. These vibrations are recorded using an optical laser, giving a dynamic measurement of texture as opposed to the quasi-static measurement given by penetrometers (Landahl and Terry, 2020). LDV is intrinsically more limited in what it can predict when compared to visNIRS, as it cannot directly evaluate the biochemical properties of an object. However, as texture is a highly important feature commercially, and is linked with many biochemical changes during fruit ripening (Zaharah et al., 2012), measuring firmness non-destructively remains incredibly valuable for the fresh produce industry. LDV gives a global measurement, in contrast with 'point' spectroscopy, which also is challenged by physiological heterogeneity in the fruit, leading to non-homogenous results. Although not previously used in mango, LDV has shown some promise in texture prediction in other crop species including avocado, onion, kiwi, apple, and persimmon (Muramatsu et al., 1999; Landahl and Terry, 2020, 2022). Since *f* is also impacted by shape and mass, the in-line implementation of this technique would require fruit to be graded before being measured, which may limit the stages of the supply chain LDV can be applied to. Similarly to visNIRS, temperature can affect the *f* measurements, which may decrease sensitivity of in-field applications (Funebo and Ohlsson, 1999). Additionally, using different cultivars may reduce accuracy, if the shape of the whole fruit and/or the internal structure (such as stone morphology) varies, similarly to the decrease in accuracy observed in visNIRS models from biochemical variation. Other impulse-response techniques (vibrometry) have been applied to mango fruit (Padda et al., 2011; Wanitchang et al., 2011). Padda et al. (2011) developed classification models that showed that acoustic measurements of *f* performed worse than hand-squeezing followed by subjective scoring for measuring firmness changes in mango.

This study aims to compare the efficacy of LDV and visNIRS as non-destructive technologies for assessing mango ripening, in order to contribute towards food loss reduction.

2. Materials and methods

2.1. Fruit material details

Mango fruit (*Mangifera indica*), cultivars 'Kent' and 'Keitt', were harvested following commercial practices, and transported to Cranfield University, UK. Mangoes were sourced and transported from Peru, Brazil and Dominican Republic, according to Table 1. After arrival at Cranfield University, fruit from each origin were evenly distributed across three sets of 260 L boxes (in triplicate; Chiltern Industrial Machining Services, UK). Peruvian fruit was cold stored during transport (21 days, 9 ± 1.5° C), while the fruit from Brazil and the Dominican Republic were air-freighted to the UK without temperature control and then cold stored (21 days, 9 ± 2° C) to mimic industry ripening conditions. After cold storage, all fruit were kept at commercial ripening conditions (20 ± 2° C and > 85% relative humidity). Fruit were acclimatised to the ripening conditions for 24 hours, before sampling every second day until past consumer acceptability (firmness values of < 1.5 N in the inner pulp). Storage times and conditions are outlined in Supplementary Figure 1. At each sampling point, ten (Peru and Dominican Republic) or eight fruit (Brazil) were removed from each 260 L ventilated box. Measurements were taken in the following order; visNIRS, LDV, colour, firmness, and TSS, followed by snap freezing in liquid nitrogen for subsequent biochemical analysis.

2.2. Reference measurements

Flesh firmness, colour, TSS and individual sugar content, were measured on mangoes at each timepoint from the equatorial region of each fruit (Fig. 1). Firmness was measured for both the 'inner' (closer to the stone) and 'outer' (closer to the skin) sections, to reflect physiological gradients in ripening. Pulp individual and total sugar content, and colour, were analysed in the 'outer' pulp, and TSS was analysed using juice from both the 'inner' and 'outer' pulp combined. Fruit were kept at 20 ± 2° C for a minimum of 24 h before measurement acquisition. Descriptive statistics of the reference measurements are outlined in Supplementary Table 2.

2.2.1. Firmness

Firmness was analysed according to Landahl and Terry (2020) with slight modifications. A 4 mm flat head cylindrical probe was mounted onto a Universal Testing Machine (68SC-05, Instron, UK) fitted with a 500 N load cell. The machine was programmed (Bluehill 2, v. 4.23, Instron, UK) such that the probe indented the sample to a depth of 5 mm with the crosshead speed at 120 mm min^{-1}. Results were reported as maximum load (Newtons, N).

2.2.2. Colour

Colour was analysed using ImageJ (v. 1.53 for Windows; National Institutes of Health, USA) on images captured by a Lumenera Infinity 3 high-definition digital camera with charge-coupled device colour sensor (Lumenera Corporation, Canada). Samples were photographed inside a Photo-e-Box plus 1419 set at D65 (6500 K) under fluorescent light tubes (back and sides) to provide consistent lighting. RGB values were measured for areas of 3–6 mm^2 and converted to L*C*h colour space (International Commission on Illumination, CIE) using standard RGB conversion equations (Easy RGB, 2018), with lightness (L*), chroma (C*), and hue angle (h°) reported.

2.2.3. Individual sugars and total soluble solids

Individual sugar extraction was based on Davis et al. (2007) with modifications. Freeze dried and powdered fruit material (50 ± 0.5 mg dry matter [DM]) was extracted using methanol/water (62.5:37.5 v/v) solution (1 mL). The mixture was heated to 55° C while shaking at 2000 rpm for 15 min (Eppendorf, Germany), before being passed through a nylon syringe filter with pore size 0.2 μm (Agilent, UK).

Table 1
Fruit sourcing details. Two mango cultivars, 'Kent' and 'Keitt' were harvested between January and September 2021. Non-destructive analyses visible and near-infrared spectroscopy (visNIRS) and laser Doppler vibrometry (LDV) were used to assess ripening.

Details of Origin	Cultivar	Number of fruit (total)	Number of sampling points	Harvest Date	Arrival to the UK	Non-destructive analyses
Parales, Peru	'Kent'	180	6	18 January 2021	16 February 2021	visNIRS and LDV
Baní, Dominican Republic	'Keitt'	150	5	12 June 2021	16 June 2021	LDV
Vale do São Francisco, Brazil	'Kent'	120	5	27 September 2021	08 October 2021	visNIRS

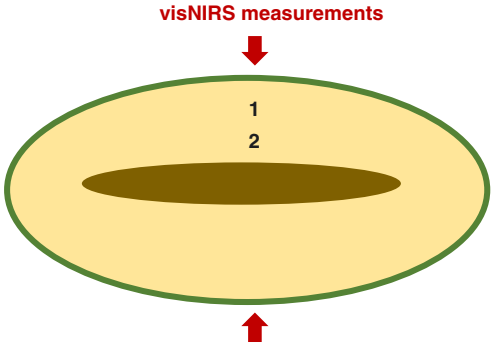


Fig. 1. Positions of destructive and non-destructive measurements taken in mango. The 'outer' (1) pulp, closer to the skin (green), and 'inner' (2) pulp , closer to the stone (brown), had separate firmness measurements to reflect gradients within the fruit. Pulp individual and total sugar content, and colour, were analysed in the 'outer' pulp (1), and TSS was analysed using juice from both the 'inner' and 'outer' pulp combined (1 and 2). The visNIR spectra were acquired at the red arrows, and the impact for the LDV was delivered to the same area.

Extracts were diluted 1:12 for pulp samples and 1:5 for skin samples, with acetonitrile/water (50:50 v/v) before analysis. Individual sugars were quantified using a High-Performance Liquid Chromatography (HPLC) system (Agilent, UK) equipped with an evaporative light scattering detector (1260 Infinity II, Agilent, UK). Extracts (20 μL) were injected into a Shodex Asahipak polymer-based column 4.6 ×250 mm, 10 nm particle size (Showa Denko America, Inc. part number NH2P-50 4E). HPLC grade water (A) and acetonitrile (B) were used as mobile phases with a flow rate of 1 mL min^{-1} programmed to the following ratios: 0 min, 20% A and 80% B; 20 min, 50% A and 50% B; 23.5 min, 20% A and 80% B, and hold until 25 min (total run time). The identity and abundance of glucose, sucrose, and fructose (individual sugars) were determined by comparing to a calibration curve constructed from Sigma-Aldrich authentic standards (UK), containing five points ranging from 0.05 to 1.25 g L^{-1}. Sugar concentrations were expressed as g kg^{-1} DM. Sum of individual sugars (SIS) was taken to be the sum of the concentrations of glucose, sucrose, and fructose (g kg^{-1} DM). The limit of detection for fructose and sucrose was 0.01 g L^{-1}, and 0.02 g L^{-1} for glucose. The limits of quantification were 0.03, 0.05, and 0.02 g L^{-1} for fructose, glucose, and sucrose respectively.

Total soluble solids (TSS) were quantified using a digital refractometer (model PR-32α, ATAGO Ltd., Japan). Juice was extracted during the firmness measurement from the same equatorial position.

2.2.4. Internal Quality Index

An internal quality index (IQI) was used to quantify ripeness in mango, as developed by Cortés et al. (2016). To investigate differences in results obtained using TSS and SIS, two versions of the IQI variable were created one using TSS, and one using SIS (mg g^{-1} DM; Eqs. 1 and 2).

$$IQI_{TSS} = \ln\left(100 \bullet Firmness \bullet L^{*} \bullet h^{*} \bullet TSS^{-1} \bullet C^{*-1}\right) \quad (1)$$

$$IQI_{SIS} = \ln\left(100 \bullet Firmness \bullet L^{*} \bullet h^{*} \bullet SIS^{-1} \bullet C^{*-1}\right) \quad (2)$$

2.3. visNIR spectral acquisition

VisNIRS reflectance measurements were taken according to Magwaza et al. (2012) with some adjustments. A LabSpec2500® Near-Infrared Analyzer (350–2500 nm; LabSpec 2500®, Analytical Spectral Devices Inc., USA) was coupled with two Peltier cooled InGaAs detectors (1000 – 1800 nm and 1800 – 2500 nm) and one Si array (350 – 1000 nm), with a sampling interval of 1 nm. Fruit skin was placed in direct contact with the fiberoptic cable, with in-built quartz-halogen light source (Ocean Optics, USA) and using reflectance mode. The system was calibrated using a Spectralon® Diffuse Reflectance Standard before starting measurements, and after every 10 fruit measured. Two points on the centre of each cheek, along the equator of the fruit (Fig. 1) were analysed. These values were averaged to obtain a single measurement per fruit.

2.4. LDV data acquisition

Laser Doppler vibrometry was used to record *f*, according to Landahl and Terry (2020) with slight modifications. Each mango was rested on a stiff sponge to stabilise the fruit, and an impact was delivered from a nylon ball on a cable tie flail (self-fabricated). A single point laser Doppler vibrometer (LV 700, Polytec UK Ltd., UK) recorded the measurements. Impacts and measurements were done on the equator of each cheek (Fig. 1). The laser light was directed at an approximately 90° angle to the impact on the fruit. Four measurements were taken for each fruit: two from the centre of each cheek. Resonant frequencies were calculated using MATLAB© (v2022b; MathWorks Inc., USA). A Fast Fourier Transform (FFT) was performed, after a high pass filter was applied (250 Hz). A moving window smoothing was applied, and the frequencies at which the first peak occurred were recorded. The four resonant frequencies per fruit were averaged to obtain a single value per fruit.

2.5. Statistics

The *f* (as measured by LDV) was compared with the destructive firmness values using Least Squares Regression Line (LSRL). The performance of each model was evaluated using the coefficient of determination (R^2) and the p-value. Both LSRL and Pearson's correlation coefficient were calculated using R© (version 4.2.0, R Foundation for Statistical Computing, Austria). While no specific cut-offs for R^2 values exist in terms of what could be implemented in-line or in-field, previous work defined R^2 values of between 0.66 and 0.81 as capable of making approximate qualitative predictions, and values above 0.82 and 0.91 capable of making good and excellent predictions, respectively. Values between 0.50 and 0.65 should be capable of distinguishing high and low values, while below 0.50 are not considered useable (Williams and Sobering, 1993; Saeys et al., 2005).

All spectral analysis was carried out using Unscrambler© (v12.2, AspenTech, Massachusetts, USA). Spectra were pre-processed, with the highest R^2s obtained by Savitzky–Golay (SG) smoothing, followed by two iterations of multiplicative scatter correction (MSC), and then 1st derivative (Savitzky and Golay, 1951; Windig et al., 2008; Supplementary Table 3). The dataset containing spectra from both origins was divided randomly into two groups; 75% for the calibration set, and 25% for the prediction set using the 'Random' function in Unscrambler

(CAMO Analytics, 2006). Partial least squares regression (PLSR) with leave one out calibration (LOOC) was used to predict each reference variable. The performance of each PLSR model is reported using the coefficient of determination for calibration (R^2_C) values, and root mean square error of calibration (RMSEC), while the predictive performances are reported using the coefficient of determination of prediction (R^2_P), the root mean square error of prediction (RMSEP), and the ratio of prediction to deviation (RPD). The RPD was calculated according to **Equation 3**, where SD is the standard deviation of the reference variable in the prediction set (Williams and Sobering, 1993). Saeys et al. (2005) classified RPD values as follows: < 1.5 is not useable, 1.5–2.0 can distinguish between high and low values, 2.0–2.5 can give approximate quantitative predictions, 2.5 – 3.0 is good, and > 3.0 is excellent. Wavelengths were selected using Martens' Uncertainty Test (CAMO Analytics, 2006) of PLSR models in Unscrambler, based on the jack-knifing principal. Additional validation of the wavelength selection was carried out through Principal Component Regression (PCR) for IQI_{SIS}, using the same wavelength selection methods.

$$RPD = SD/RMSEP \quad (3)$$

3. Results

3.1. Predicting internal quality attributes using visNIRS

In skin tissue, the highest R^2 value was found for predicting glucose content ($R^2_P = 0.810$), with poor predictions for other individual and total sugars ($R^2_P = 0.476$, 0.508, and 0.521 for fructose, sucrose, and SIS, respectively; Table 2, Supplementary Figure 2) using 'Kent' fruit from Peru and the Dominican Republic. For the pulp, glucose again had the highest R^2 value among the individual sugars ($R^2_P = 0.656$) compared to the others ($R^2_P = 0.363$–0.582). While the model for TSS had a similar R^2 value to that obtained for pulp glucose ($R^2_P = 0.639$), TSS and SIS correlated poorly in mangoes from both harvests (Pearson's r = 0.456; Fig. 2, Supplementary Table 4).

The firmness predictions were poor for both the inner and outer pulp ($R^2_P < 0.5$; Table 2). Each of the predictions for colour (L*, C*, and h°)

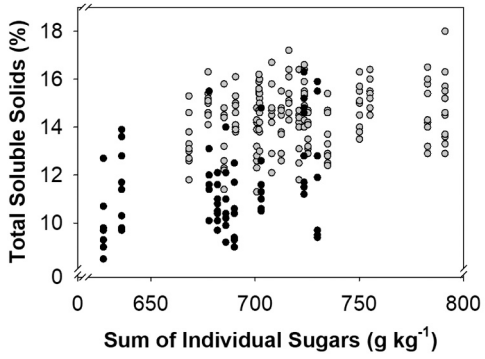


Fig. 2. Sum of the individual sugar content *vs.* total soluble solids of mango pulp. Fruit from Peru (grey) and Brazil (black) do not show strong correlation between total sum of the individual sugars (SIS) and TSS (%). SIS is the sum of the glucose, sucrose, and fructose concentrations (g kg^{-1} DM).

Table 2
Prediction models for mango quality attributes using visNIRS. The quality of the visNIRS models for variables including individual sugars, the sum of the individual sugars (SIS), total soluble solids (TSS), firmness, colour values (i.e. lightness [L*], chroma [C*], and hue angle [h°]), and the internal quality indices (IQIs) are summarised using the coefficient of determination of calibration and prediction (R^2_C and R^2_P, respectively), the root mean square errors of calibration and prediction (RMSEC and RMSEP, respectively), and the ratio of prediction to deviation (RPD).

Variables		Calibration		Prediction		
Variable	Tissue	R_C^2	RMSEC	R_P^2	RMSEP	RPD
Fructose	Skin	0.691	14.460	0.476	19.002	1.392
Glucose	Skin	0.889	7.968	0.810	9.990	2.312
Sucrose	Skin	0.683	22.544	0.508	26.468	1.437
SIS	Skin	0.687	40.069	0.521	47.364	1.456
Fructose	Outer Pulp	0.857	7.595	0.582	10.734	1.560
Glucose	Outer Pulp	0.788	7.911	0.656	10.304	1.718
Sucrose	Outer Pulp	0.788	19.284	0.570	27.893	1.537
SIS	Outer Pulp	0.685	20.554	0.363	29.635	1.263
TSS	Pulp	0.751	1.027	0.639	1.126	1.676
Firmness	Outer Pulp	0.723	4.768	0.479	5.759	1.396
Firmness	Inner Pulp	0.596	5.188	0.454	6.274	1.364
L*	Outer Pulp	0.725	9.933	0.555	12.234	1.511
C*	Outer Pulp	0.728	12.431	0.603	16.404	1.599
h°	Outer Pulp	0.737	5.600	0.408	7.790	1.309
IQI_{TSS}	Outer Pulp	0.863	0.431	0.670	0.586	1.757
IQI_{SIS}	Outer Pulp	0.902	0.375	0.729	0.532	1.937

variables had low R^2 values ($R^2_P = 0.555$, 0.603, and 0.408, respectively) and low RPD values (RPD = 1.511, 1.599, 1.309).

The internal quality indices (IQI_{TSS} and IQI_{SIS}) gave some of the highest R^2_Ps (0.670 and 0.729 respectively; Table 2), each with acceptable RPD values (1.757 and 1.937 respectively. Including SIS rather than TSS in the calculation of IQI increased the R^2 and RPD values, and decreased the RMSEP (Fig. 2).

The lowest RMSEP values were produced as a function of the variables IQI_{SIS} (0.532) IQI_{TSS} (0.586), and TSS (1.126). These values were similar to those found calculating the RMSEC for these variables (IQI_{SIS} [0.375], IQI_{TSS} [0.431], and TSS [1.027]), showing the reliability of the PLSR calibration and prediction models developed.

3.2. Predicting firmness using LDV

The *f* of fruit from two cultivars, 'Kent' (Peru) and 'Keitt' (Dominican Republic) was used to predict the firmness measured destructively in both the inner and outer pulp (Table 3). All predictions using both cultivars ('Kent' [Peru] and 'Keitt' [Dominican Republic]) had low R^2 values, even without being divided into calibration and prediction sets ($R^2 < 0.35$), as seen in Table 3. Marginal increases were seen when using 'Keitt' fruit only ($R^2 = 0.477$). The decrease in *f* through time was linear (Pearson's r = −0.65; Fig. 3**A**) while the destructive firmness measurement showed an exponential decrease (Fig. 3**B**).

Table 3
The predictive ability of resonant frequency (*f*), as measured by LDV, for the outer and inner pulp firmness (OP and IP, respectively) of mango fruit. Predictive ability was quantified using least squares regression line (LSRL) with the average of the four *f* measurements taken per fruit. To account for non-linear relationships, the natural log (ln) of the firmness value (for exponential functions) or both the outer (OP) and inner pulp (IP) firmness and *f* (for power functions) were compared.

Origin	Cultivar	Comparison		R^2	p-value
Both origins	'Kent' and 'Keitt'	OP firmness	*f*	0.2698	< 0.001
		IP firmness	*f*	0.2756	< 0.001
		ln(OP firmness)	*f*	0.3358	< 0.001
		ln(IP firmness)	*f*	0.3025	< 0.001
		ln(OP firmness)	ln (*f*)	0.3436	< 0.001
		ln(IP firmness)	ln (*f*)	0.3043	< 0.001
Peru	'Kent'	OP firmness	*f*	0.3088	< 0.001
		IP firmness	*f*	0.3713	< 0.001
		ln(OP firmness)	*f*	0.2816	< 0.001
		ln(IP firmness)	*f*	0.3048	< 0.001
		ln(OP firmness)	ln (*f*)	0.2963	< 0.001
		ln(IP firmness)	ln (*f*)	0.3218	< 0.001
Dominican Republic	'Keitt'	OP firmness	*f*	0.2446	< 0.001
		IP firmness	*f*	0.2099	< 0.001
		ln(OP firmness)	*f*	0.4682	< 0.001
		ln(IP firmness)	*f*	0.4768	< 0.001
		ln(OP firmness)	ln (*f*)	0.4625	< 0.001
		ln(IP firmness)	ln (*f*)	0.4764	< 0.001

4. Discussion

4.1. Prediction performance of visNIRS is better for TSS than SIS

Historically, most of the visNIRS ripening prediction models in mango have used TSS as 'Y' variable because it was assumed to be a good indicator of sugar content (Hahn and Hernandez, 2005; Blasco et al., 2016; Cortés et al., 2016; Maraphum et al., 2022). However, our results showed that TSS and SIS are not correlated in mango fruit from either origin (Pearson's r = 0.456; Fig. 4, Supplementary Table 4) suggesting that TSS is a poor indicator for sugar content. This discrepancy is linked to TSS measurements also including non-carbohydrates, such as proteins and amino acids (Kusumiyati et al., 2020), which can vary independently of individual sugars.

In our work, we compared predictions for TSS to individual and SIS (the sum of the individual sugars glucose, sucrose, and fructose). While the highest R^2_P value (0.810) was obtained for individual glucose prediction in the skin, this is not a highly consumer-valued trait, as the skin is not eaten. The prediction for glucose in the pulp ($R^2_P = 0.656$) was worse than for the skin, likely due to limited light reaching the pulp after passing through the skin. By contrast, the predictions for the other individual sugars in the skin (sucrose and fructose), and in the pulp, as well as SIS, were not useable. The model for predicting TSS performed similarly to the one for pulp glucose prediction (R^2_P of 0.639), meaning it was better predicted than most individual sugars, and the SIS of the pulp. This result is similar to Delwiche et al. (2008), who found that in mango, the NIR region better predicted TSS than any of the sugars individually, or the SIS content ($R^2 = 0.88$ for TSS, and $R^2 = 0.67 – 0.75$ for individual sugars, and $R^2 = 0.82$ for the sum). An additional consideration is the cost and time associated with quantifying individual sugar content, which is considerably more expensive than measuring TSS (Magwaza and Opara, 2015). Whether this increased cost would be worthwhile will depend on many factors, including the amount of waste produced within that stage of the supply chain, and the value of the end product (where a higher value may be associated with some products, e.g. fresh-cut mango, and lower costs for fruit used for juices and smoothies).

4.2. Prediction performance for IQI/ripeness was improved by using SIS

Using IQI may better reflect ripeness than any one individual variable, as IQI incorporates colour, firmness, and sweetness properties (Cortés et al., 2016). When TSS and SIS were predicted as independent variables, TSS had a higher R^2_P and lower RMSEP compared to SIS. However, when including TSS and SIS as sweetness indicators in IQI calculations (**Equations 1** and **2**), IQI_{SIS} had a higher R^2 and lower RMSEP than IQI_{TSS}. The R^2_P values obtained in this study for IQI prediction ($R^2_P = 0.670–0.729$) are lower than that developed by Cortés et al. (2016; $R^2_P = 0.879$), but included fruit from two origins and harvest seasons, which could reduce our model accuracy. However, including multiple origins and harvest seasons truly represents the context that would be experienced in real-world situations and increases robustness against biological variation (Rungpichayapichet et al., 2016). These results suggested that incorporating SIS, rather than TSS, could improve the prediction of mango ripeness using visNIRS. This improvement is in spite of the individual measurements (one value per fruit) taken for TSS, and the mixed measurements taken for sugars (fruit were grouped pooled into 10 [for Peru] and eight [for Brazil] and an average value applied to each of the spectra in that group).

Using SIS, or individual sugars, over TSS in ripening prediction has additional advantages. Individual sugars are signalling molecules, and can impact the physiological changes during ripening (Durán-Soria et al., 2020). For example, sucrose promotes colour change through carotenoid accumulation (Télef et al., 2006, Iglesias et al., 2001). Another potential benefit of using SIS over TSS is improving sweetness prediction. Since the perceived fruit sweetness by consumers varies

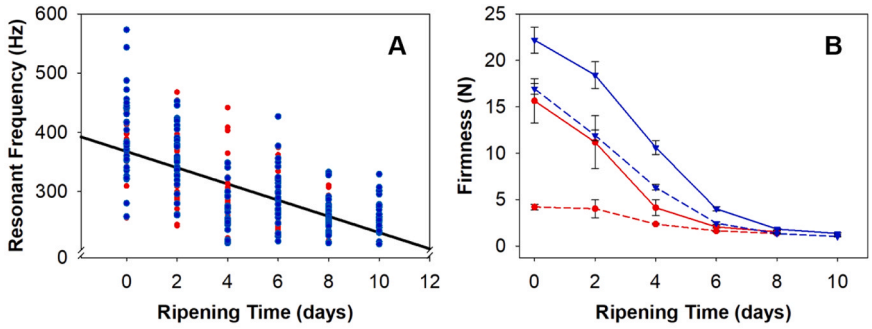


Fig. 3. Relationships between the resonant frequency (A) and destructively measured firmness (B). A: Linear correlation between resonant frequency, measured by LDV, and ripening time in 'Kent' (blue) and 'Keitt' (red) mangoes. Pearson's correlation coefficient indicated a negative linear correlation, with $r = -0.65$ and $p < 0.001$. **B:** Approximately exponential decreases are seen through time for both the inner (dashed) and outer (solid) pulp firmness in 'Kent' (blue) and 'Keitt' (red) mangoes.

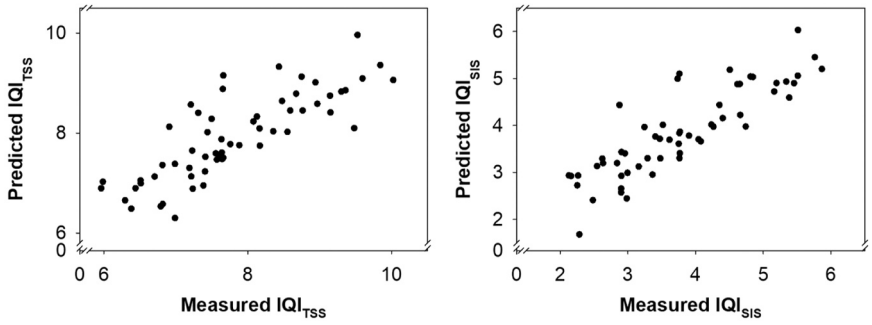


Fig. 4. Predicted *vs*. measured values for internal quality index (IQI) attributes using visNIRS. Models were created using 'Kent' mangoes from Peru and the Dominican Republic.

between glucose, sucrose, and fructose (Mouillot et al., 2019; Moskowitz, 1970), predicting these independently could allow relative sweetness to be factored into future prediction models. However, since current commercial practice for retailers is to use TSS to determine the acceptability of fruit (Valente et al., 2011), the decision to move away from TSS and prioritise actual sugar content would need to be made jointly between producers and retailers to prevent unnecessary rejection of acceptable quality produce and avoid waste.

4.3. Targeted wavelengths can increase cost-effectiveness

In this study, a large number of wavelengths and spectral regions were covered: the visible (*ca.* 350 – 750 nm), NIR (*ca.* 750 – 1100 nm), and short-wave infrared spectrum (*ca.* 1100 – 2500 nm). In order to analyse this spectral range, several detectors are needed, and the data analysis is computationally intensive. These requirements make the commercial use of this method costly; therefore, to make implementation more affordable, it is common to identify the most important wavelengths associated with each variable, and only analyse those selected regions, both to reduce detector cost and the dimensionality of the data to increase processing speed (Walsh et al., 2020; Cortés et al., 2016). However, for predicting IQI_{SIS}, when important wavelengths were selected using the weighted regression coefficients, 41% of the spectra contributed significantly to the model, which spanned the majority of the range used (382–2423 nm). The weighted regression coefficients for predicting IQI_{SIS} and the selected important wavelengths are shown in Supplementary Figure 3**, A and C**. A similar result was obtained from using PCR, where a large proportion of the spectra were selected using Marten's Uncertainty Test (Supplementary Figure 3**, B and D**). The use of alternative regression models (e.g. Multiple Linear Regression) or machine learning methods, and alternative feature selection methods (e.g. forward selection) might improve the overall performance of the models and the wavelength selection process (Mishra and Woltering, 2023; Mishra and Passos, 2021; Mishra and Nikzad-Langerodi, 2020; Liu et al., 2008). However, it is also possible that since IQI incorporates several variables (colour, SIS, and firmness) the regions associated with each factor may not overlap, giving a larger number of wavebands than expected for a single variable.

4.4. Predicting texture: a complex trait

A limitation of sound and vibration models is that they can only be linked to textural properties, hence can struggle in predicting other ripening-related traits including colour changes, and biochemical profiles. This constraint may limit estimates of ripeness when compared to visNIRS. However, firmness is not only a highly consumer-valued and commercially important trait, but associated to fruit ripening; therefore, it is worthwhile to predict.

The prediction of firmness using visNIRS was poor ($R^2_P < 0.5$; Table 2) for both the inner and outer pulp, but might be improved through alternative regression methods, as previously achieved by Mishra et al. (2020), and alternative pre-processing methods, as outlined by Purwanto et al. (2015). Using interval PLSR, Mishra et al. (2020) showed a 14% reduction in prediction error, indicating that different data processing and analysis methods can be chosen to enhance the performances of models for different variable predictions. The highest R^2 value reported for firmness predicted by visNIRS is 0.99 (Watanawan et al., 2014), but this model did not include fruit from more than one region or harvest season, and compared the predicted TSS value from a handheld NIR spectrometer to the penetrometer firmness (not directly comparing the spectra to the firmness variable).

The LDV model for firmness produced similar results to that of visNIRS, with R^2 values of < 0.5 in each case. This result indicated these models are not useable. That said, the LDV model faced an additional

challenge compared to the visNIRS, as they contained two cultivars ('Kent' and 'Keitt'), which may have been a factor in the lower model performances (Rungpichayapichet et al., 2016). Higher R^2 results were obtained using 'Keitt' fruit only, which may suggest that the structure of the fruit might be more amenable for LDV analysis. This difference could be due to there being less variability in shape within the 'Keitt' fruit – either due to the grading process or genetic determination of shape. It may also reflect differences in the morphology and connectivity between the skin, pulp, and stone in each cultivar (Majumder et al., 2011). However, when training the LDV models based on one cultivar, only a small number of samples were available (n = 180 for 'Kent', and n = 150 for 'Keitt'), which is likely also a limiting factor in the models' accuracies. In addition to size and shape, moisture content of the fruit also affects impulse response measurements (Funebo and Ohlsson, 1999), which can vary across cultivars and harvest seasons (Anderson et al., 2020). A drop in moisture content is measured as a softening of tissue and could mask the ripening induced softening. The heterogenic pulp firmness within each mango cheek provides an additional challenge for LDV models. Previous work has shown that the less fleshy side of mango fruit gave a higher firmness estimate, attributable to the increased contribution from the seed to the overall measure (Al-Haq and Sugiyama, 2004).

Penetrometers measure the force required to insert a probe of a specific size into the pulp to a certain depth. The resonant frequencies are the characteristic or natural vibrating frequencies of a body or a system determined by the physical parameters of the vibrating object. The *f* can be related to the stiffness (S) of a sphere through the following equation (Landahl and Terry, 2020; Eq. 4):

$$S = f^2 * m^{2/3} \quad (4)$$

Interestingly, since the *f* decreases linearly with time, and the destructive (quasi-static) firmness measurement decreased exponentially, these results suggest that the destructive and vibrational methods of assessing texture are quantifying distinct physiological characteristics. Stiffness is proportional to elasticity; therefore, it is more related to the resistance to a slight squeeze of tissue, rather than the break of the tissue during compression. This result is supported by Subedi and Walsh (2009), who found a similar disconnect between penetrometer firmness and sound velocity. Texture, while heavily influenced by firmness and elasticity, is a complex trait that is difficult to translate from consumer experience into a quantitative value. Notably, Valente et al. (2009) showed that visNIRS predictions of mango firmness were improved when texture was measured using vibrations, rather than destructively. Some of the highest reported R^2 values from the literature use *f* measurements to measure firmness for visNIRS model creation (Kasim et al., 2021; Mishra et al., 2020). However, since the retailers typically use penetrometer firmness as their quality measure (Padda et al., 2011; Valente et al., 2011), this could lead to rejection of fruit that have been classified as acceptable by these models.

LDV has not been applied to measure firmness in mango previously, but other vibrational techniques have been used to predict firmness with varying levels of success (Padda et al., 2011; Subedi and Walsh, 2009; Al-Haq and Sugiyama, 2004; Mizrach et al., 1999). Padda et al. (2011) found that their acoustic measurements of *f* were outperformed by hand-squeezing followed by subjective scoring for measuring firmness changes in mango. Mizrach et al. (1999) reported an R^2 of 0.64 using the passage of ultrasonic waves through mangoes, when predicting penetrometer firmness. They reported better results (R^2 = 0.67 – 0.87) for predicting TSS, acidity, and storage time than penetrometer firmness, further supporting that vibrational and penetrometer measurements quantify distinct fruit characteristics. Other studies using acoustic technologies on mango measured the sound velocity, rather than *f*, which gave much higher R^2 values (0.8 – 0.989) when predicting penetrometer firmness (Subedi and Walsh, 2009; Al-Haq and Sugiyama, 2004) than those obtained in this study. It is therefore possible that mangoes are better suited to the use of sound velocity, rather than resonant frequency, as non-destructive methods of assessing firmness.

LDV models could also incorporate damping estimates; however, these have been shown to not be valuable measures in highly viscoelastic materials, such as avocado flesh, instead showing effectiveness in predicting onion textural changes linked to pathological deterioration (Landahl and Terry, 2020, 2022). Another alternative approach would be to use LDV in tandem with another non-destructive technique (such as visNIRS), to improve the performance of the prediction models. Valente et al. (2009) used this sensor fusion approach with visNIRS and an acoustic measure of stiffness in mango, but did not use predictions reliable enough for use in industry (R^2 = 0.541). By contrast, Wanitchang et al. (2011) used an acoustic measure in combination with the visible spectrum, specific gravity, size, impact response, and sphericity of mango fruit to develop a model capable of classifying 95% of fruit into the correct maturity class. However, the time and cost associated with obtaining all of these measurements would be higher than visNIRS alone, and the categories predicted refer to fruit developmental stages (immature, mature, and overmature), rather than ripening progression. Zakaria et al. (2012) also used sensor fusion with an acoustic sensor coupled to an electronic nose system to improve the classification of mango into ripening stages. Neither of Zakaria et al. (2012), Wanitchang et al. (2011), nor Valente et al. (2009) discussed predictions using the acoustic measurements independently of the other measures, and so results cannot be directly compared to those obtained in this study. Since sensor fusion would come at an increased investment cost and maintenance requirements, it is likely that improvements to the optical visNIRS technique (through machine learning, additional spectral pre-processing, and wavelength selection) would be a better investment than including an additional non-destructive technique for mango ripeness prediction, depending on computational intensity. However, as infrastructure and equipment availability evolve in the global food chain, this may be a strong application in the future.

5. Conclusions

The non-destructive prediction of mango ripening characteristics was evaluated by both visNIRS and LDV. The best prediction model for mango ripeness was found using visNIRS to predict IQI, which includes colour, sweetness, and firmness variables. The prediction of IQI was improved by using SIS as a sweetness estimate, rather than TSS. This improvement is in spite of the mostly poor predictions of individual sugars in the pulp. This approach gives the added benefit of better reflecting the consumer-valued 'sweetness' of a fruit, as SIS and TSS did not correlate well. The IQI_{SIS} model also included fruit from different harvest seasons and origins, reflecting industry conditions. The predictions of firmness by LDV were poor for both cultivars investigated, suggesting that it is not a viable alternative for measuring ripeness to visNIRS. This result is likely due to the distinct characteristics quantified by destructive methods (e.g. penetrometer and texturometer) and vibrometry. An optimised handling of visNIRS data and the acceptance of an IQI using SIS content has the potential to improve homogeneity and reduce waste within the mango import, ripening, and fresh-cut industries. Further research into the relationship between vibrational attributes (*f* and sound velocity) and consumer experience in mango fruit may lead to improved quality assessments and reduced food waste.

Funding

This work was funded by Orchard House Foods Ltd. and Cranfield University through the Cranfield Industrial Partnership PhD Scheme.

Declaration of Competing Interest

The authors declare that they have no known competing financial interests or personal relationships that could have appeared to influence

the work reported in this paper.

Data Availability

Data underlying this study can be accessed at http://doi.org/10.17862/cranfield.rd.25381456.

Acknowledgements

This work was funded by Orchard House Foods Ltd. and Cranfield University through the Cranfield Industrial Partnership PhD Scheme. The authors would like to thank David Talbot and Janey Cawsey from Orchard House Foods Ltd. for their technical support.

Author contributions

M.C.A., S.K. and L.A.T. were responsible for the project resources. M.C.A., N.F., S.K. and C.O.B. conceived and designed the experiments. C.O.B carried out the experiments, and performed data collection and analyses. The original draft was written by C.O.B., which was then edited and reviewed by all authors. Project administration was done by M.C.A., and project supervision was carried out by M.C.A, N.F., and S.K.

Appendix A. Supporting information

Supplementary data associated with this article can be found in the online version at doi:10.1016/j.postharvbio.2024.112878.

References

Al-Haq, M.I., Sugiyama, J., 2004. Measurement if firmness of Irwin mangoes by a non-destructive acoustic tester during cold storage. Trans. ASABE 47 (6). https://doi.org/10.13031/2013.17790.

Anderson, N.T., Walsh, K.B., Subedi, P.P., Hayes, C.H., 2020. Achieving robustness across season, location and cultivar for a NIRS model for intact mango fruit dry matter content. Postharvest Biol. Technol. 168, 1–9. https://doi.org/10.1016/j.postharvbio.2020.111202.

Beckles, D.M., 2012. Factors affecting the postharvest soluble solids and sugar content of tomato (Solanum lycopersicum L.) fruit. Postharvest Biol. Technol. (1), 129–140. https://doi.org/10.1016/j.postharvbio.2011.05.016.

Blasco, J., Lorente, D., Cortes, V., Talens, P., Cubero, S., Munera, S., Aleixos, N., 2016. Application of near infrared spectroscopy to the quality control of citrus fruits and Mango. NIR N. 27 (7), 4–7. https://doi.org/10.1255/nirn.1637.

Bobelyn, E., Serban, A.S., Nicu, M., Lammertyn, J., Nicolai, B.M., Saeys, W., 2010. Postharvest quality of apple predicted by NIR-spectroscopy: study of the effect of biological variability on spectra and model performance. Postharvest Biol. Technol. 55 (3), 133–143. https://doi.org/10.1016/j.postharvbio.2009.09.006.

CAMO Analytics. (2006). The Unscrambler Methods - CAMO Software.

Cortés, V., Blanes, C., Blasco, J., Ortíz, C., Aleixos, N., Mellado, M., Cubero, S., Talens, P., 2017. Integration of simultaneous tactile sensing and visible and near-infrared reflectance spectroscopy in a robot gripper for mango quality assessment. Biosyst. Eng. 162, 112–123. https://doi.org/10.1016/j.biosystemseng.2017.08.005.

Cortés, V., Ortiz, C., Aleixos, N., Blasco, J., Cubero, S., Talens, P., 2016. A new internal quality index for mango and its prediction by external visible and near-infrared reflection spectroscopy. Postharvest Biol. Technol. 118, 148–158. https://doi.org/10.1016/j.postharvbio.2016.04.011.

Davis, F., Terry, L.A., Chope, G.A., Faul, C.F.J., 2007. Effect of extraction procedure on measured sugar concentrations in onion (Allium cepa L.) bulbs. J. Agric. Food Chem. 55 (11), 4299–4306. https://doi.org/10.1021/jf063170p.

Delwiche, S.R., Mekwatanakarn, W., Wang, C.Y., 2008. Soluble solids and simple sugars measurement in intact mango using near infrared spectroscopy. HortTechnology 18 (3), 410–416. https://doi.org/10.21273/HORTTECH.18.3.410.

Durán-Soria, S., Pott, D.M., Osorio, S., Vallarino, J.G., 2020. Sugar signalling during fruit ripening. Front. Plant Sci. 11, 1–18. https://doi.org/10.3389/fpls.2020.564917.

FAO, 2018. Food loss analysis: causes and solutions - case study on the mango value chain in the Republic of India. Rome 58 pp..

Funebo, T., Ohlsson, T., 1999. Dielectric properties of fruits and vegetables as a function of temperature and moisture content. J. Micro Power Electro Energy 34 (1), 42–54. https://doi.org/10.1080/08327823.1999.11688387.

Gupta, A.K., Medhi, M., Chakraborty, S., Yumnam, M., Mishra, P., 2021. Development of rapid and non-destructive technique for the determination of maturity indices of pomelo fruit (Citrus grandis). J. Food Meas. Charact. 15 (2), 1463–1474. https://doi.org/10.1007/s11694-020-00734-4.

Hahn, F., Hernandez, G., 2005. Comparison of maturity detection of "Ataulfo" mangoes using thermal imaging and NIR. EFITA/WCCA Jt. Congr. 1, 229–235.

Hale, T.A., Hassell, R.L., Phillips, T., 2005. Refractometer measurements of soluble solid concentration do not reliably predict sugar content in sweet corn. HortTechnology 15 (3), 668–672. https://doi.org/10.21273/HORTTECH.15.3.0668.

Harker, F.R., Marsh, K.B., Young, H., Murray, S.H., Gunson, F.A., Walker, S.B., 2002. Sensory interpretation of instrumental measurements 2: sweet and acid taste of apple fruit. Postharvest Biol. Technol. 24 (3), 241–250. https://doi.org/10.1016/S0925-5214(01)00157-0.

Helstad, S., 2019. Corn Sweeteners. in Corn (Third Edition). AACC International Press,, pp. 551–591. https://doi.org/10.1016/B978-0-12-811971-6.00020-6.

Gómez, Hernández, Wang, J, A., García Pereira, A., 2005. Impulse response of pear fruit and its relation to Magness-Taylor firmness during storage. Postharvest Biol. Technol. 35 (2), 209–215. https://doi.org/10.1016/j.postharvbio.2004.07.006.

Iglesias, D.J., Tadeo, F.R., Legaz, F., Primo-Millo, E., Talon, M., 2001. In vivo sucrose stimulation of colour change in citrus fruit epicarps: Interactions between nutritional and hormonal signals. Physiol. Plant. 112 (2), 244–250. https://doi.org/10.1034/j.1399-3054.2001.1120213.x.

Kasim, N.F.M., Mishra, P., Schouten, R.E., Woltering, E.J., Boer, M.P., 2021. Assessing firmness in mango comparing broadband and miniature spectrophotometers. Infrared Phys. Technol. 115 https://doi.org/10.1016/j.infrared.2021.103733.

Landahl, S., Terry, L.A., 2020. Non-destructive discrimination of avocado fruit ripeness using laser Doppler vibrometry. Biosyst. Eng. 194, 251–260. https://doi.org/10.1016/j.biosystemseng.2020.04.001.

Landahl, S., Terry, L.A., 2022. Detection of internal defects in onion bulbs by means of single-point and scanning laser Doppler vibrometry. Biosyst. Eng. 221, 258–273. https://doi.org/10.1016/j.biosystemseng.2022.07.004.

Lebrun, M., Plotto, A., Goodner, K., Ducamp, M.N., Baldwin, E., 2008. Discrimination of mango fruit maturity by volatiles using the electronic nose and gas chromatography. Postharvest Biol. Technol. 48 (1), 122–131. https://doi.org/10.1016/j.postharvbio.2007.09.010.

Liu, S., Huang, H., Huber, D.J., Pan, Y., Shi, X., Zhang, Z., 2020. Delay of ripening and softening in 'Guifei' mango fruit by postharvest application of melatonin. Postharvest Biol. Technol. 163, 1–9. https://doi.org/10.1016/j.postharvbio.2020.111136.

Liu, Y., Chen, X., Ouyang, A., 2008. Nondestructive determination of pear internal quality indices by visible and near-infrared spectrometry. LWT - Food Sci. Technol. 41 (9), 1720–1725. https://doi.org/10.1016/j.lwt.2007.10.017.

Magwaza, L.S., Opara, U.L., 2015. Analytical methods for determination of sugars and sweetness of horticultural products-A review. Sci. Hortic. 184, 179–192. https://doi.org/10.1016/j.scienta.2015.01.001.

Magwaza, L.S., Opara, U.L., Terry, L.A., Landahl, S., Cronje, P.J., Nieuwoudt, H., Mouazen, A.M., Saeys, W., Nicolaï, B.M., 2012. Prediction of "Nules Clementine" mandarin susceptibility to rind breakdown disorder using Vis/NIR spectroscopy. Postharvest Biol. Technol. 74, 1–10. https://doi.org/10.1016/j.postharvbio.2012.06.007.

Majumder, D.A.N., Hassan, L., Rahim, M.A., Kabir, M.A., 2011. Studies. physio-Morphol., Flor. Biol. Fruit. Charact. mango. J. Bangladesh Agric. Univ. 9 (2), 187–199. https://doi.org/10.22004/ag.econ.208638.

Maraphum, K., Ounkeaw, A., Kasemsiri, P., Hiziroglu, S., Posom, J., 2022. Wavelengths selection based on genetic algorithm (GA) and successive projections algorithms (SPA) combine with PLS regression for determination the soluble solids content in Nam-DokMai mangoes based on near infrared spectroscopy. Eng. Appl. Sci. Res 49 (1), 119–126. https://doi.org/10.14456/easr.2022.14.

Mishra, P., Nikzad-Langerodi, R., 2020. Partial least square regression versus domain invariant partial least square regression with application to near-infrared spectroscopy of fresh fruit. Infrared Phys. Technol. 111, 1–7. https://doi.org/10.1016/j.infrared.2020.103547.

Mishra, P., Passos, D., 2021. A synergistic use of chemometrics and deep learning improved the predictive performance of near-infrared spectroscopy models for dry matter prediction in mango fruit. Chemom. Intell. Lab. Syst. 212, 1–8. https://doi.org/10.1016/j.chemolab.2021.104287.

Mishra, P., Woltering, E., 2023. Semi-supervised robust models for predicting dry matter in mango fruit with near-infrared spectroscopy. Postharvest Biol. Technol. 200, 1–9. https://doi.org/10.1016/j.postharvbio.2023.112335.

Mishra, P., Woltering, E., El Harchioui, N., 2020. Improved prediction of 'Kent' mango firmness during ripening by near-infrared spectroscopy supported by interval partial least square regression. Infrared Phys. Technol. 110, 1–6. https://doi.org/10.1016/j.infrared.2020.103459.

Mizrach, A., Flitsanov, U., Schmilovitch, ev, Fuchs, Y., 1999. Determination of mango physiological indices by mechanical wave analysis. Postharvest Biol. Technol. 16 (2), 179–186. https://doi.org/10.1016/S0925-5214(99)00007-1.

Moskowitz, H.R., 1970. Ratio scales of sugar sweetness. Percept. Psychophys. 7, 315–320. https://doi.org/10.3758/BF03210175.

Mouillot, T., Barthet, S., Janin, L., Creteau, C., Devilliers, H., Brindisi, M.C., Penicaud, L., Leloup, C., Brondel, L., Jacquin-Piques, A., 2019. Taste perception and cerebral activity in the human gustatory cortex induced by glucose, fructose, and sucrose solutions. Chem. Senses 44 (7), 435–447. https://doi.org/10.1093/chemse/bjz034.

Munawar, A.A., Hörsten, D., Mörlein, D., Pawelzik, E., Wegener, J.K., 2013. Rapid and non-destructive prediction of mango sweetness and acidity using nearinfrared spectroscopy. Proc. - Ser. Ges. Inform. (GI) 211.

Muramatsu, N., Sakurai, N., Wada, N., Yamamoto, R., Tanaka, K., Asakura, T., Ishikawa-Takano, Y., Nevins, D.J., 1999. Remote Sensing of Fruit Textural Changes with a Laser Doppler Vibrometer. J. Am. Soc. Hortic. Sci. 125 (1), 120–127. https://doi.org/10.21273/JASHS.125.1.120.

Munera, S., Amigo, J.M., Blasco, J., Cubero, S., Talens, P., Aleixos, N., 2017. Ripeness monitoring of two cultivars of nectarine using VIS-NIR hyperspectral reflectance imaging. J. Food Eng. 214, 29–39. https://doi.org/10.1016/j.jfoodeng.2017.06.031.

Munera, S., Blasco, J., Amigo, J.M., Cubero, S., Talens, P., Aleixos, N., 2019. Use of hyperspectral transmittance imaging to evaluate the internal quality of nectarines. Biosyst. Eng. 182, 54–64. https://doi.org/10.1016/j.biosystemseng.2019.04.001.

Nordey, T., Léchaudel, M., Génard, M., Joas, J., 2014. Spatial and temporal variations in mango colour, acidity, and sweetness in relation to temperature and ethylene gradients within the fruit. J. Plant Physiol. 171 (17), 1555–1563. https://doi.org/10.1016/j.jplph.2014.07.009.

Padda, M.S., do Amarante, C.V.T., Garcia, R.M., Slaughter, D.C., Mitcham, E.J., 2011. Methods to analyze physico-chemical changes during mango ripening: A multivariate approach. Postharvest Biol. Technol. 62 (3), 267–274. https://doi.org/10.1016/j.postharvbio.2011.06.002.

Purwanto, Y.A., Sari, H.P., Budiastra, W., 2015. Effects of preprocessing techniques in developing a calibration model for soluble solid and acidity in "Gedong Gincu" mango using NIR spectroscopy. Int. J. Eng. Technol. 7 (5), 1921–1927. ⟨https://www.researchgate.net/publication/287222610⟩.

Rungpichayapichet, P., Mahayothee, B., Nagle, M., Khuwijitjaru, P., Müller, J., 2016. Robust NIRS models for non-destructive prediction of postharvest fruit ripeness and quality in mango. Postharvest Biol. Technol. 111, 31–40. https://doi.org/10.1016/j.postharvbio.2015.07.006.

Saeys, W., Mouazen, A.M., Ramon, H., 2005. Potential for onsite and online analysis of pig manure using visible and near infrared reflectance spectroscopy. Biosyst. Eng. 91 (4), 393–402. https://doi.org/10.1016/j.biosystemseng.2005.05.001.

Savitzky, A., Golay, M.J.E., 1951. Smoothing and Differentiation of Data by Simplified Least Squares Procedures. Anal. Chem. 36 (8), 1627–1639. https://doi.org/10.1021/ac60214a047.

Silué, Y., Nindjin, C., Cissé, M., Kouamé, K.A., Amani, N. guessan G., Mbéguié-A-Mbéguié, D., Lopez-Lauri, F., Tano, K., 2022. Hexanal application reduces postharvest losses of mango (Mangifera indica L. variety "Kent") over cold storage whilst maintaining fruit quality. Postharvest Biol. Technol. 189, 1–6. https://doi.org/10.1016/j.postharvbio.2022.111930.

Silva, A.P.F.B., Do Nascimento, J.R.O., Lajolo, F.M., Cordenunsi, B.R., 2008. Starch mobilization and sucrose accumulation in the pulp of keitt mangoes during postharvest ripening. J. Food Biochem. 32 (3), 384–395. https://doi.org/10.1111/j.1745-4514.2008.00175.x.

Subedi, P.P., Walsh, K.B., 2009. Non-invasive techniques for measurement of fresh fruit firmness. Postharvest Biol. Technol. 51 (3), 297–304. https://doi.org/10.1016/j.postharvbio.2008.03.004.

Télef, N., Stammitti-Bert, L., Mortain-Bertrand, A., Maucourt, M., Carde, J.P., Rolin, D., Gallusci, P., 2006. Sucrose deficiency delays lycopene accumulation in tomato fruit pericarp discs. Plant Mol. Biol. 62 (3), 453–469. https://doi.org/10.1007/s11103-006-9033-y.

Thanaraj, T., Terry, L.A., Bessant, C., 2009. Chemometric profiling of pre-climacteric Sri Lankan mango fruit (*Mangifera indica* L. Food Chem. 112, 786–794. https://doi.org/10.1016/j.foodchem.2008.06.040.

Valente, M., Leardi, R., Self, G., Luciano, G., Pain, J.P., 2009. Multivariate calibration of mango firmness using vis/NIR spectroscopy and acoustic impulse method. J. Food Eng. 94 (1), 7–13. https://doi.org/10.1016/j.jfoodeng.2009.02.020.

Valente, M., Ribeyre, F., Self, G., Berthiot, L., Assemat, S., 2011. Instrumental and sensory characterization of mango fruit texture. J. Food Qual. 34 (6), 413–424. https://doi.org/10.1111/j.1745-4557.2011.00412.x.

Walsh, K.B., Blasco, J., Zude-Sasse, M., Sun, X., 2020. Visible-NIR 'point' spectroscopy in postharvest fruit and vegetable assessment: The science behind three decades of commercial use. Postharvest Biol. Technol. 168, 1–17. https://doi.org/10.1016/j.postharvbio.2020.111246.

Wanitchang, P., Terdwongworakul, A., Wanitchang, J., Nakawajana, N., 2011. Non-destructive maturity classification of mango based on physical, mechanical and optical properties. J. Food Eng. 105 (3), 447–484. https://doi.org/10.1016/j.jfoodeng.2011.03.006Get.

Watanawan, C., Wasusri, T., Srilaong, V., Aree, W.-, Kanlayanarat, S., 2014. Near infrared spectroscopic evaluation of fruit maturity and quality of export Thai mango (Mangifera indica L. var. Namdokmai). Food Res. Int. 21 (3), 11109–11114.

Williams, P.C., Sobering, D.C., 1993. Comparison of Commercial near Infrared Transmittance and Reflectance Instruments for Analysis of Whole Grains and Seeds. J. Infrared Spectrosc. 1 (1), 25–32. https://doi.org/10.1255/jnirs.3.

Windig, W., Shaver, J., Bro, R., 2008. Loopy MSC: A Simple Way to Improve Multiplicative Scatter Correction. Appl. Spectrosc. 62 (10), 1153–1159. https://doi.org/10.1366/000370208786049097.

Zaharah, S.S., Singh, Z., Symons, G.M., Reid, J.B., 2012. Role of Brassinosteroids, Ethylene, Abscisic Acid, and Indole-3-Acetic Acid in Mango Fruit Ripening. J. Plant Growth Regul. 31 (3), 363–372. https://doi.org/10.1007/s00344-011-9245-5.

Zakaria, A., Shakaff, Md, Masnan, A.Y., Saad, M.J., Adom, F.S.A., Ahmad, A.H., Jaafar, M.N., Abdullah, M.N., H, A., L. M, Kamarudin, 2012. Improved maturity and ripeness classifications of Magnifera Indica cv. harumanis mangoes through sensor fusion of an electronic nose and acoustic sensor. Sensors 12 (5), 6023–6048. https://doi.org/10.3390/s120506023.



https://dspace.org/

Non-destructive methods for mango ripening prediction: visible and near-infrared spectroscopy (visNIRS) and laser Doppler vibrometry (LDV)

O'Brien, Ciara; Falagán, Natalia; Kourmpetli, Sofia; Landahl, Sandra; Terry, Leon A. ...

2024-06-01
Elsevier
https://doi.org/10.1016/j.postharvbio.2024.112878
O'Brien C, Falagán N, Kourmpetli S, et al., (2024) Non-destructive methods for mango ripening prediction: visible and near-infrared spectroscopy (visNIRS) and laser Doppler vibrometry (LDV). Postharvest Biology and Technology, Volume 212, June 2024, Article Number 112878

Downloaded from a DSpace repository. https://dspace.org/